



Evidence for the Late Cretaceous Asteroussia event in the Gondwanan Ios basement terranes

Sonia Yeung¹, Marnie Forster¹, Emmanuel Skourtsos², Gordon Lister¹

¹ Structure Tectonics Team, Research School of Earth Sciences, Australian National University, Canberra, 2601 Australia

5 ² Section of Dynamic, Tectonic and Applied Geology, Department of Geology and Geoenvironment, National and Kapodistrian University of Athens, Athens 157 72, Greece

Correspondence to: Sonia Yeung (HoSonia.Yeung@anu.edu.au)

10 **Abstract.** ⁴⁰Ar/³⁹Ar geochronology on garnet-mica schists and the underlying Gondwanan granitoid basement terrane on Ios demonstrates evidence of a Late Cretaceous high pressure, medium temperature (HP–MP) metamorphic event. This suggests that the Asteroussia crystalline nappe on Crete may extend northward and include Ios, in the Cyclades. If this is correct, the northern part of the Asteroussia nappe (on Ios) is overlain by the terrane stack defined by the individual slices of the Cycladic Eclogite-Blueschist Unit, whereas in the south (in Crete) the Asteroussia nappe is at the top of a nappe stack defined by the
15 individual tectonic units of the external Hellenides. This geometry implies that the accretion of the Ios basement terrane involved a significant leap (250–300 km) southwards of the surface outcrop of the subduction megathrust. This accretion would have commenced at or about ~38 Ma, when the already exhumed terranes of the Cycladic Eclogite-Blueschist Unit had begun to thrust over the Ios basement. By ~35 Ma, we suggest the subduction jump had been accomplished, and renewed rollback began the extreme extension that led to the exhumation of the Ios metamorphic core complex.

20 1 Introduction

Our previous research (e.g., Forster and Lister, 2009; Forster et al., 2020) suggests the existence of a Late Cretaceous metamorphic event affecting the basement rocks on Ios, Cyclades, Aegean Sea, Greece (Fig. 1). Metamorphic events with the same age are present in klippen recognised in small outcrops around the Asteroussia mountains in Crete and later defined as a major component of the Attic-Cycladic Crystalline Belt (Be'eri-Shlevin et al., 2009; Dürr et al., 1978; Seidel et al., 1976).
25 Previously published papers considered the Asteroussia terrane as relicts of a high-temperature, low-pressure (HT-LP) granitoid-dominated unit with peak metamorphic conditions in the Late Cretaceous ~70 Ma (Altherr et al., 1994; Be'eri-Shlevin et al., 2009; Langosch et al., 2000). The Asteroussia event also affected other higher-level tectonic slices in the Cyclades



(Be'eri-Shlevin et al., 2009). Rather than the previous interpretation of dates as ‘excess argon’ or ‘mixing age’, we demonstrate that the Ios basement terranes experienced a Late Cretaceous Asteroussia event associated with high-pressure metamorphism, specifically with the growth of phengitic mica in the augengneiss terrane and the overlying garnet-mica schist.

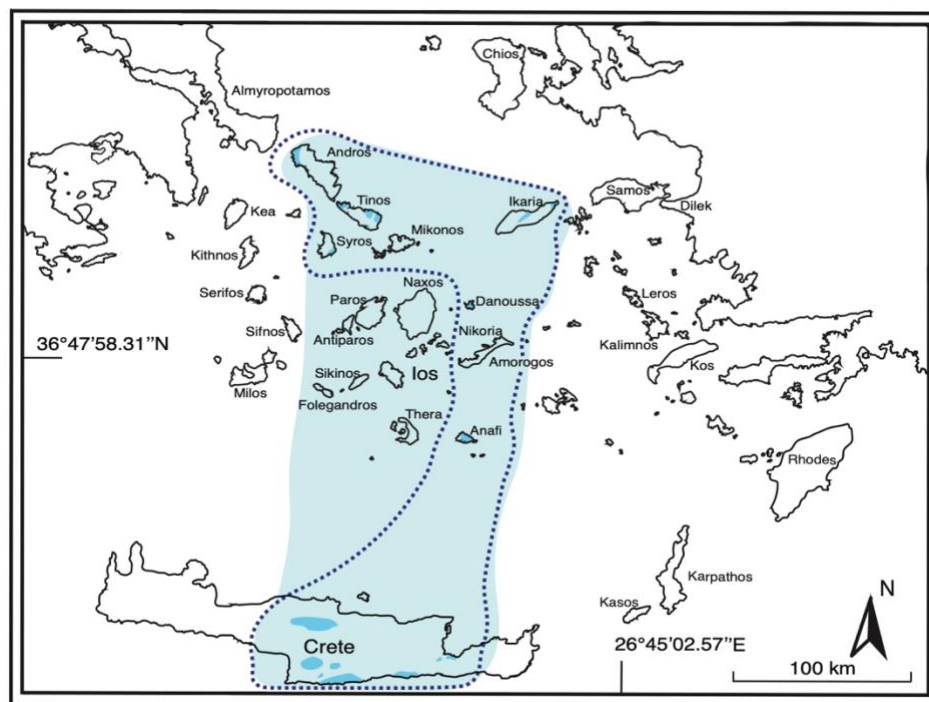
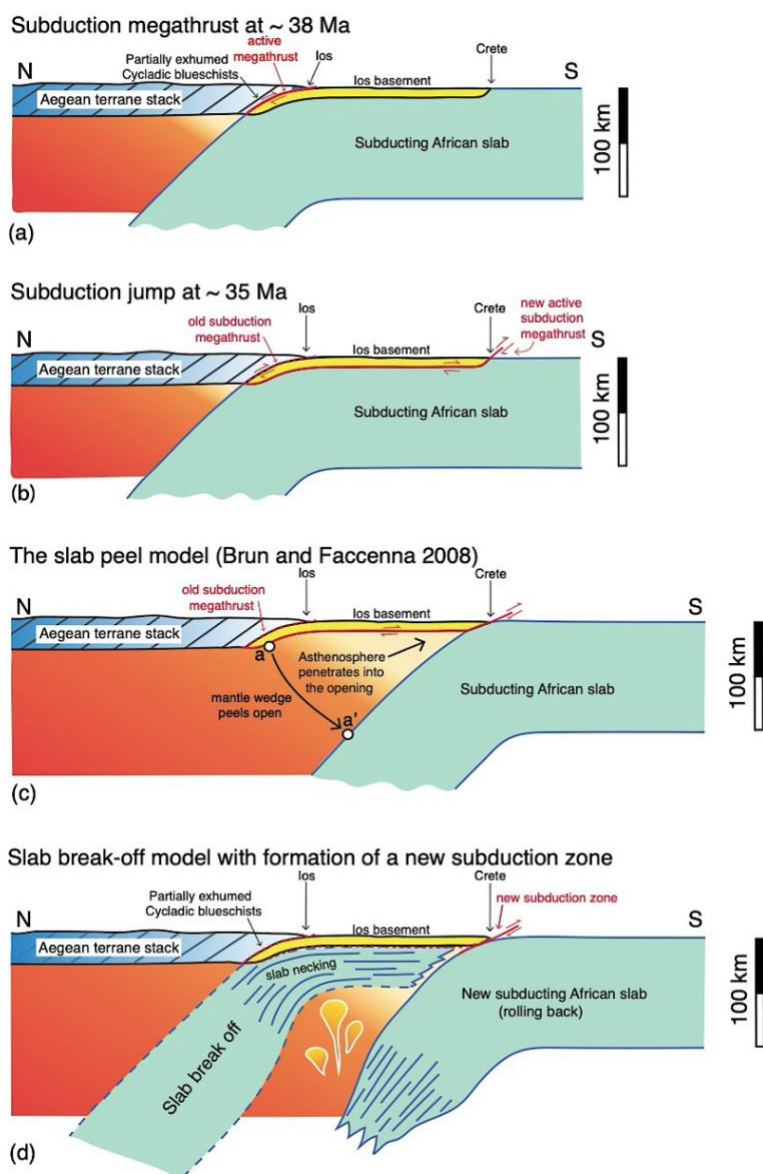


Figure 1: Map of the Cyclades and Crete, dotted line illustrates published extent of the Asteroussia nappe; area shaded in black are localities of outcrops with late Cretaceous age. (information retrieved from Be'eri-Shlevin et al., 2009). Area shaded in light blue is the revised extent of the Asteroussia nappe suggested by this paper.

Figure 1 shows the areal extent of the Asteroussia terrane based on Be'eri-Shlevin et al. (2009), with the shaded area indicating the revised extent according to what we report in this paper. If correct, this is a significant modification, for it implies a widespread metamorphic event in northern Tethys during Late Cretaceous time. Moreover, if the extent of the basement terrane is as large as indicated in Fig. 1, its accretion to the modern terrane-stack in latest Eocene time implies a southward jump of the subduction zone megathrust exceeding 250–300 km (Figs. 2a and 2b). Potentially this requires these terranes to have been autochthonous, with their final accretion involving a period of flat slab subduction followed by the initiation of a new subduction zone (Fig. 2d). Subsequent rollback can then stretch the Cycladic crust, explaining the variation in crustal thickness



from ~32 km thick beneath the Cyclades, to 18 km beneath the Sea of Crete, and ~ 30 km beneath Crete (based on Makris and Vees, 1976 and Makris et al., 2001) as due to stretching subsequent to the Late Eocene accretion event that included Ios.



45 **Figure 2: Schematic cross-sections illustrating controversial models of deep crustal material exhumation in Central Aegean region.**
 (a) Accretion of the Ios basement to the terrane stack through subduction megathrust operation involved a period of flat slab
 subduction (Africa plate) at ~ 38 Ma time. (b) Step 2 subduction megathrust operation after (a) at ~ 35 Ma time. This is the period
 during which a subduction ‘jump’ occurred. (c) The ‘slab peel’ model described by Brun and Faccenna (2008) is a possible model
 explaining how Aegean tectonics evolved from (a) to (b). But this model implies a wide-spread occurrence of melting due to the rising
 50 asthenosphere, yet melting was not as extensive in the Cyclades. (d) The three-staged ‘slab break off’ model is more accurate in



Aegean tectonics by addressing how the terrane stack was subjected to overall stretching with some evidences of melting such as plutonic intrusions in centre of metamorphic core complexes.

2 The Asteroussia Nappe

The Asteroussia nappe was first identified in Crete, at the top of the local terrane stack, where it reflects the imprint of metamorphism in the time range 70–80 Ma (Bonneau, 1972; Bonneau, 1984). Later, the terrane was characterised as having Late Cretaceous high-temperature low-pressure (HT-LP) metamorphic assemblages associated with granitoid intrusions (Dürr et al., 1978; Langosch et al., 2000; Patzak et al., 1994; Seidel et al., 1976). Other researchers then reported outcrops with the same metamorphic age, all occurring as small klippen on various Cycladic islands (Tinos, Andros, Syros, Donoussa, Ikaria, Nikouria and Anafi) as well as on Crete (Avigad and Garfunkel, 1989; Be'eri-Shlevin et al., 2009; Bröcker and Franz, 2006; Dürr et al., 1978; Langosch et al., 2000; Patzak et al., 1994; Seidel et al., 1976). Be'eri-Shlevin et al. (2009) then extended the Asteroussia nappe to cover a north-south distance of ~300 km (Fig. 1), noting that although published Rb-Sr dates of the Asteroussia nappe range from ~45–85 Ma, the dates cluster at ~70 Ma.

However, in the Cyclades, the Late Cretaceous event in the upper unit of the terrane stack occurs in meta-ophiolites and mélangé that experienced blueschist facies metamorphism overprinted by low-pressure greenschist facies (Avigad and Garfunkel, 1989; Be'eri-Shlevin et al., 2009; Bröcker and Franz, 1998; Bröcker and Franz, 2006; Pe-Piper and Photiades, 2006). This upper unit (meta-ophiolite and mélangé) overlies units that preserve evidence of high-pressure metamorphism overprinted by a later crustal stretching deformation event, with no Asteroussian dates reported (Avigad and Garfunkel, 1989; Be'eri-Shlevin et al., 2009; Bröcker and Franz, 1998; Bröcker and Franz, 2006; Pe-Piper and Photiades, 2006; Ring et al., 2003). Most published island-scale structural models involve 2 to 4 tectonic slices. In contrast the Asteroussia outcrops in Crete are small (up to 10-15 km wide) tectonic klippen with poor lithological and structural correlations (Dürr et al., 1978; Seidel et al., 1976; Seidel et al., 1981). Nevertheless, Be'eri-Shlevin et al. (2009) argue that the different outcrops in the north (Andros, Tinos, Syros, Ikaria) and in the south (Ikaria, Donoussa, Nikouria, Anafi) Cycladic islands are part of an extensive Asteroussian nappe that once extended northward from Crete.



75 **2.2 The Asteroussia event on Ios?**

Overall, the island of Ios is marked by the outcrop of a terrane stack with thin tectonic slices separated by island-scale deformation structures such as detachment faults and/ or ductile shear zones. All terranes experienced Early Oligocene stretching and were variably affected by the south-directed South Cyclades Shear Zone (SCSZ). An Eocene-Oligocene high pressure terrane (the upper plate of the Ios Detachment) overlies the Gondwanan basement terrane (Kaey and Lister, 2002).

80 The tectonic slices forming the upper plate include marble, schists and gneisses with high pressure assemblages above the Ios detachment (e.g., Forster and Lister 1999a, b; Forster and Lister, 2009; Forster et al., 2020; Huet et al., 2009; Huet et al., 2011; Ring et al., 2007). The lower plate consists of three tectonic slices (or slivers) in which garnet-mica schist and augengneiss are the major lithologies (e.g., Andriessen et al., 1987; Baldwin and Lister, 1998; Forster and Lister, 2009; Vandenberg and Lister, 1996).

85

Forster and Lister (2009) reported $^{40}\text{Ar}/^{39}\text{Ar}$ dates at ~70-80 Ma on white mica in deformation fabrics in the augengneiss. This led us to speculate that the Ios lower plate was made up of garnet-mica schist and augengneiss that could also be part of the Asteroussia nappe. However, we need to demonstrate that the 70–80 Ma date reported in the structurally deepest augengneiss of the Ios lower plate was in fact the characteristic ‘Asteroussia age’ rather than the previously speculated ‘excess argon’ or
90 ‘mixing age’. Therefore, we set out to examine outcrops on Ios, focusing on the north-west corner of the basement terranes in an attempt to determine the meaning of the previously reported 70-80 Ma ages. We combined a field study with microstructural analysis and $^{40}\text{Ar}/^{39}\text{Ar}$ geochronology to address: i) the character and location of micro-deformation structures with late Cretaceous age on Ios; ii) the time relationships between various metamorphic and deformation events.

95 This new $\text{Ar}^{40}/\text{Ar}^{39}$ geochronology data was collected using furnace-based step heating experiments, and once again identified Asteroussian ages in Ios basement rocks, especially in the garnet-mica schist unit. These ages are preserved in phengitic white mica which appears to be highly retentive of radiogenic argon. Therefore, we were able to demonstrate the timing of metamorphic mineral growth under high pressure conditions in Late Cretaceous time.



3 Microstructural analysis and mineral chemistry

100 The Ios lower plate is made up of three tectonic slices each with different metamorphic histories. The domed, south-directed South Cyclades Shear Zone (SCSZ) is prominent in the higher level of the lower plate and marks the tectonic contact between the upper and lower units of the Ios terrane stack (Fig. 3). The Port Beach tectonic slice is the structurally highest level of the lower plate, immediately beneath the Ios detachment. This tectonic slice consists of a fault-bounded, complexly folded tectonic silvers of garnet-mica schist overlaying a augengneiss tectonic silver with quartz micro-boudins. The thick garnet-mica schist
105 unit beneath the Port Beach tectonic slice is the structural mid-level whereas the augengneiss core of the Ios metamorphic core complex defines the structurally deepest level in Ios terrane stack.

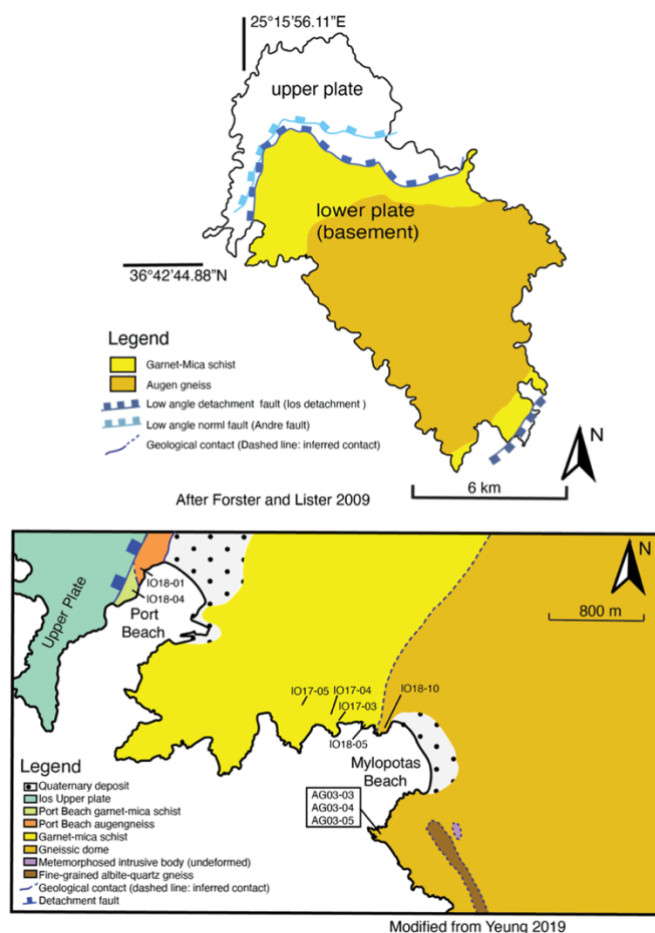


Figure 3: Top: island-scale map illustrating major lithology. Bottom: Detailed map of study area with sample collection indicated in blue stars. Diagrams after Yeung (2019).



110

Field observations in these two lower units identified evidence for multiple alternating (and overprinting) deformation events such as recumbent folds and extensional shear zones. Detailed analysis of overprinting microstructures produced relative time constraints using the method of Tectonic Sequence Diagrams (TSDs, after Forster and Lister (2008)). Outcrops of both tectonic slivers in the structurally highest Port Beach tectonic slice preserved numerous recumbently folded veins, isoclinal folds and boudinage structures formed under crustal extension. A section of altered, greenschist facies garnet-mica schist with chloritoid replacing garnets was observed near the tectonic contact between Ios upper and lower plate.

115

TABLE 1 – LIST OF SAMPLES

Sample number (rock type)	location		Mineral(s) dated	Measured ages
	Lat (°N)	Long (°E)		
<u>Port Beach tectonic slice (structurally highest in Ios lower plate)</u>				
	36°42.9'N			
IO18-01 (augengneiss)		25°17.2'E	White mica first generation white mica, likely pre-deformation grains	192 ± 1.3 Ma 188 ± 1.0 Ma 84.2 ± 2.3 Ma
			K-feldspar crystals in groundmass	592 ± 8.7 Ma 166 ± 2.8 Ma 39.8 ± 3.5 Ma
<u>Mylopotas tectonic slice (structurally mid-level in Ios lower plate)</u>				
IO17-03* (garnet-mica schist)	36°42.9'N	25°17.2'E	White mica south-directed shear zone deformation fabrics	76.9 ± 0.7 Ma 36.0 ± 0.5 Ma
IO17-04 (garnet-mica schist)	36°42.9'N	25°17.2'E	White mica south-directed shear zone deformation fabrics	163 ± 1.0 Ma 174 ± 1.1 Ma



IO17-05 *† (garnet-mica schist)	36°42.9'N	25°17.2'E	White mica south-directed shear zone deformation fabrics	81.0 ± 0.6 Ma 58.8 ± 1.5 Ma
IO18-05 † (garnet-mica schist)	36°42.5'N	25°17.2'E	White mica south-directed shear zone deformation fabrics structurally lowest level of this tectonic unit	50.7 ± 0.4 Ma 43.8 ± 1.1 Ma

Augengneiss basement (structurally lowest in Ios lower plate)

Samples published in Forster and Lister (2009); data reviewed in this study

AG03-03§ (augengneiss)	36°42.2'N	25°17.2'E	White mica South-directed shear zone deformation fabrics overprinted by north-directed shear zone K-feldspar Groundmass and porphyroclasts subjected to south-directed then north-directed sense of shear	73.9 ± 0.6 Ma 70.4 ± 0.8 Ma 84.8 ± 0.7 Ma ~ 13 ± 0.1 Ma
AG03-05 (augengneiss)	36°42.2'N	25°17.3'E	White mica South-directed shear zone deformation fabrics overprinted by north-directed shear zone	72 ± 0.6 Ma 68.3 ± 0.3 Ma

Note: Samples are stored in the collections of the Structure Tectonics Team, Research School of Earth Sciences, Australian National University, Canberra, 2601 Australia

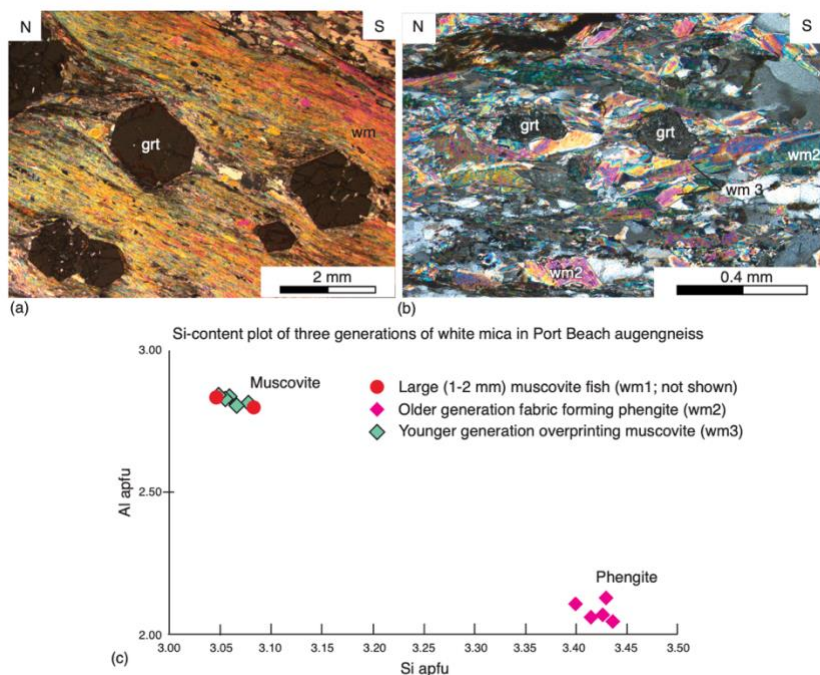
* Rock sample preserved evidences of eclogite facies after the first (deformation) fabric

† The younger age is comparable with the Δ_{1B} eclogite event in Syros

§ Age derived from the lower limit of a saddle-shaped apparent age spectrum



Samples selected included a basement augengneiss (IO18-01) with a pervasive south-directed shear fabrics, and four samples
120 (IO17-03, IO17-05, IO17-04, IO18-05) from the deformed garnet-mica schist underplating the Port Beach tectonic slice. These
samples display different textures and different generations of mineral growth. Samples IO17-03 and IO17-04 display earliest
formed garnets as large as 2–3 cm in diameter. Sample IO18-05 represents the structurally lowest level of this tectonic unit.
We note that metabasite was observed sporadically in the augengneiss basement, and that the minerals assemblages such that
125 it was subject to transitional greenschist-blueschist metamorphism during the Δ_{1D} event of Forster et al. (2020). The protolith
is likely to have been intermediate-mafic intrusive dykes that folded and deformed with the country rock. Haematite nodes are
found in the top three metres of an intense shear zone at the contact between overplating garnet-mica schist and this basement
augengneiss. This indicates the presence of fluid at the contact of these two juxtaposed tectonic slices. The prominent structural
contact between the garnet-mica schist and the augengneiss is defined by a late-developed intense north-sense shear zone.

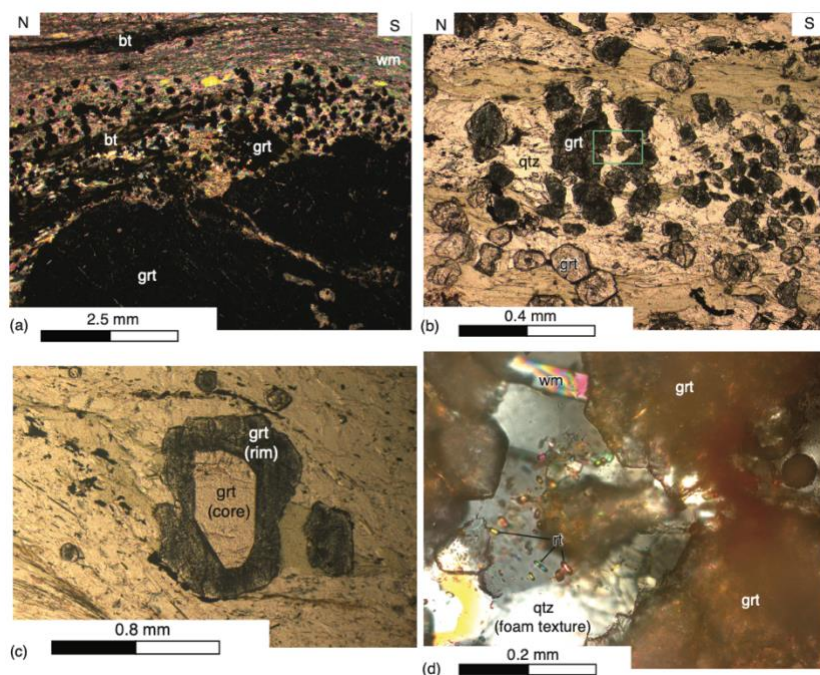


130 **Figure 4: Microstructures analysis on the Port Beach tectonic slice. (a) δ -type garnet porphyroblasts in Port Beach garnet-mica schist. (b) Two generations of overprinted white mica deformation fabrics, with elongated grains (indicated by black lines) overprinting ones with a 'lens' shape (indicated by white index). (c) Si-content plot illustrating the presence of phengite and muscovite in the Port Beach augengneiss, the older, lens-shaped white micas are identified as phengite whereas the younger, elongated grains are muscovite. The large mica porphyroclasts are muscovite.**

135



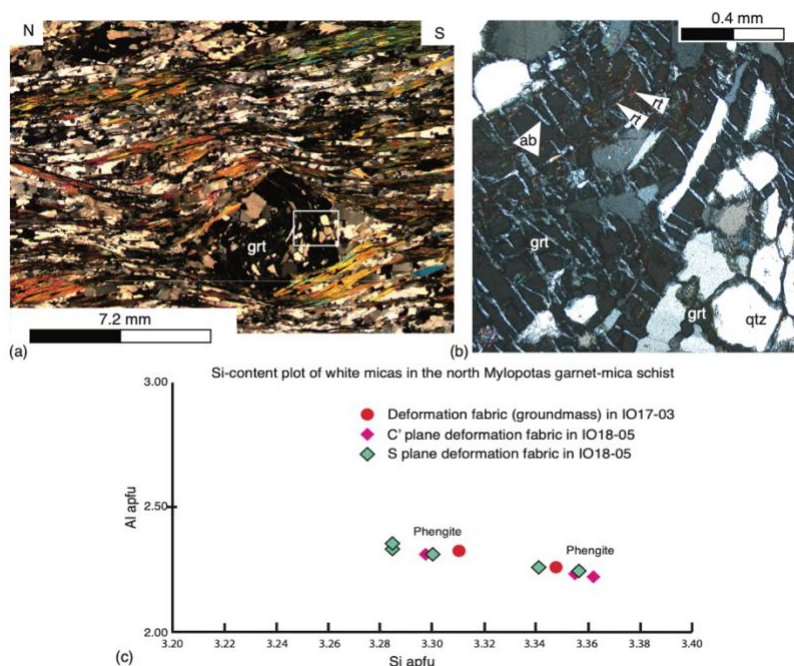
Both the garnet-mica schist and the augengneiss tectonic silvers in Port Beach tectonic slice were affected by south-directed shearing. Garnet porphyroblasts grown over pervasive white mica fabrics were later rotated and deformed to δ -type clasts (Passchier and Simpson, 1986) in the Port Beach garnet-mica schist (Fig. 4a). No large K-feldspar porphyroclasts are observed in the Port Beach augengneiss. Instead, small (5-10 mm) quartz ‘mini-boudins’ appear to have been nucleated in voids created
140 by the shearing. Three white mica generations were observed, including pre-mylonite porphyroblasts (now present as muscovite fish with dynamically recrystallised rims) and younger, recrystallised muscovite that intergrew with dynamically recrystallised K-feldspar and quartz (Fig. 4b). Mineral chemistry identified large white mica grains as muscovite, whereas the groundmass mica is phengite with silicate content (Si-content) suggesting P-T conditions of 100-140 MPa and 500-600°C (Fig. 4c) (cf. Massonne and Schreyer, 1987; Patrick, 1995; Velde, 1967). Small garnets are preserved in low-strain zones in the
145 shear zone, particularly adjacent to pull-apart voids later filled by quartz (Fig. 4b). We conclude that the Port Beach tectonic slice was subjected to higher pressure metamorphic conditions than have been previously suggested.



150 **Figure 5: Microstructure analysis on the garnet-mica schist tectonic slice. (a) White mica dominated deformation fabric with minor biotite relict of early fabric surrounds large 2–3 cm diameter garnets, younger 2–3 mm garnets grow on the deformation fabric. (b) Thin section under plane polarized light: two types small, second generation garnets with different chemical compositions are identified. (c) A slightly larger (~ 4mm diameter) second generation garnet with a zoned crystalline texture. (d) magnified view of the green box in (b), euhedral second-generation garnet grew into a quartz foam texture with relict rutile floating in the void space.**



Three generations of garnet growth are observed in sample IO17-03 where all garnets are non-end-member minerals with chemistries similar to almandine. These non-end-member crystals are low in calcium, significantly high in iron and slightly higher magnesium when compared to end-member almandine. The 2–3 cm diameter garnets are formed earlier: younger, 2–3 mm diameter crystals are light red or black (Fig. 5a, 5b). Several younger 5–8 mm diameter garnets have a zoned mineral growth in which the core is light red (Ca depleted, Mn enriched) and the rim is black (Mn depleted, Ca enriched) (Fig. 5c). Dynamically recrystallized, south-sense white mica fabric wraps around the larger garnet porphyroblasts, with second generation garnets growing over this fabric. Traces of rutile crystals ‘float’ in the foam-textured quartz adjacent to garnet porphyroclasts (Fig. 5d). Microstructures in sample IO17-04 are similar, with first generation, 1–2 cm diameter garnets fragmented by shear zone operation. South-directed shearing was more intense in sample IO17-05, with a single generation garnet porphyroblasts observed and surrounded by recrystallised white mica and quartz. These data suggest a higher-pressure history than has previously been recognised.

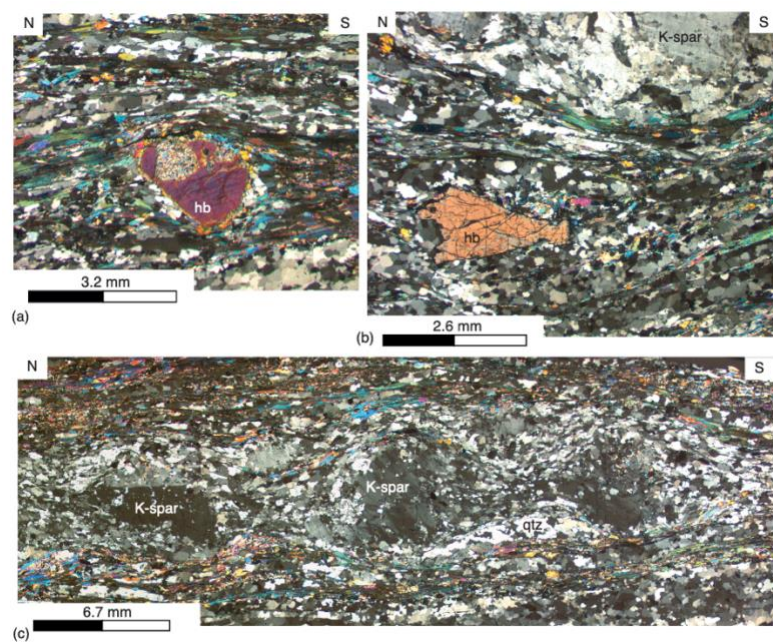


165

Figure 6: (a) Garnet porphyroblast preserving relicts of earlier deformation fabrics as inclusions and developed a skeletal structure once it reached the Al-depleted zone. (b) Rutile inclusions and albite exsolution trails observed in the garnet porphyroblast. (c) Si-content plot indicates presence of two phengite groups in the garnet-mica schist unit.



170 The earliest microstructure in sample IO18-05 is a white mica fabric with rutile inclusions preserved as inclusions within 5–8
mm garnet porphyroblasts. These non-end-member garnet porphyroblasts nucleated on Al-rich white mica during early shear
zone operation and continued to grow during deformation until they reached the Al-depleted, foam-textured quartz in pressure
shadows. The fluids then corroded grain-boundaries, developing a skeletal structure in new grown garnet in which the original
foam texture in the incorporated quartz grains can still be recognised (Fig. 6b, bottom right corner). The garnet porphyroblasts
175 are rotated during shear zone operation, as inferred from the oblique angle between white mica–rutile inclusion and the
recrystallised groundmass (Fig. 6a, showing the core of a garnet porphyroblast). Dynamic recrystallisation of white mica and
quartz in the groundmass occurred synchronously during shear zone operation. Other microstructures of interest preserved in
IO18-05 are the first order grey albite trails in fractures through the large garnet porphyroblasts (Fig. 6b) and a series of sheared
haematite nodules that grew on white mica, but have no relative time correlation to garnets. The Si-content of white micas in
180 sample IO17-03 and IO18-05 (both as mixture of muscovite and phengite) suggests that the phengite grew under P-T condition
up to 500-1000 MPa and 400-500°C (Fig. 6c). Thus the structurally mid-level garnet-mica schist tectonic slice also recorded
a complex history of deformation and metamorphism with evidence of high-pressure eclogite-facies metamorphism.



185 **Figure 7: Microstructures analysis on the south Mylopotas headland augengneiss. (a) an older generation white mica preserved as large porphyroclasts wrapped by younger, recrystallized white mica. (b) K-feldspar porphyroclasts with minor recrystallisation limited to the edge and a hornblende xenocryst preserved in low strain zone. (c) K-feldspars porphyroclasts overprinted by both the earlier south-directed shear zone and the younger north-directed shear zone, forming ‘micro boudin’ structure whilst maintaining its crystal structure in the core area.**



190 Augengneiss in the basement contains large K-feldspar xenocrysts preserved as porphyroclasts. Samples analysed in this study were deformed by the south-directed South Cyclades Shear Zone (SCSZ) then variably overprinted by narrow north-directed shear zones. K-feldspar porphyroclasts surrounded by dynamically recrystallised white mica and quartz in these sample were fractured by shearing, with recrystallisation at the edges (Fig. 7b). A single hornblende porphyroclast wrapped by a south-sense white-mica shear fabric was observed in AG03-04 (Fig. 7a, thin-section parallel to the stretching lineation). Pre-
195 deformation hornblende was also observed in low-strain zones adjacent to K-feldspar porphyroclasts (Fig. 7b). The youngest microstructure observed in these samples is the quartz filled cracks created by crustal stretching. The augengneiss basement records evidence of recumbent folding during crustal shortening, followed by ductile stretching under a south-directed shear zone. All of this occurred before the augengneiss was juxtaposed against the garnet-mica schist slice by an intense north-directed shear zone.

200 **4 Argon geochronology**

Argon geochronology was performed on white mica from deformation fabrics and on the K-feldspar porphyroclasts. Details of specific microstructure(s) dated and the ages obtained are summarised in Table 1. Data from the south Mylopotas headland augengneiss samples AG03-03 and AG03-05 have previously been published by Forster and Lister (2009) but these samples have been re-examined here so and that data is also included.

205

White mica, especially the phengites from the garnet-mica schist and underlying augengneiss, is an ideal mineral to perform microstructurally focused $^{40}\text{Ar}/^{39}\text{Ar}$ geochronology. In this study white micas are key to identifying evidence for older Asteroussian structures that have been overprinted by younger Alpine events. Quantitative furnace-based step heating $^{40}\text{Ar}/^{39}\text{Ar}$ geochronology experiments under ultra-high vacuum (UHV) were performed on white micas from several samples,
210 with grain sizes ranging from 250 μm to 355 μm . The apparent age spectra produced varied in their character depending on the structural character and rock type. For example, differently shaped argon spectra were obtained from the garnet-mica schist and the augengneiss and are quite distinct. The phengitic white micas from the garnet-mica schist produced a spectrum with a characteristic ‘hump-shaped’ partial plateau. Whereas age spectra produced by phengitic white mica in the underlying



augengneiss generally produced spectra with a partial plateau followed by a peak at the last heating steps. It is important to
215 note that the shear zones operated in this area operated in the Argon Partial Retention Zone (Ar PRZ; details in Forster and
Lister, 2009), and the complex age spectra preserve and record the effect of multiple deformation and metamorphic mineral
growth events. To help with the interpretation of the complex age spectra, the results were analysed and modelled using
specifically designed computer software *eArgon* and *MacArgon* (details in Forster and Lister, 2004; Forster and Lister, 2010;
Forster et al., 2014; Forster et al., 2015; Lister and Baldwin, 1996). The method of asymptote and limit was used to delineate
220 end-member ages from the age spectra, since most steps are affected by mixing of argon populations (Forster and Lister, 2004;
Forster and Lister, 2009)

The argon geochronology analyses yielded age clusters in Early-Middle Jurassic, Late Cretaceous, Eocene–Oligocene and
Oligocene–Miocene time (Table 1). However, the evidence for Jurassic and Cretaceous ages is exclusively restricted to argon
225 populations retained in phengite, or, in the case of IO18-01, to the large muscovite fish. All white mica analysed yielded
Arrhenius plots that unequivocally demonstrate both phengite and muscovite components, e.g., IO17-05 in the garnet-mica
schist, and AG03-03 in the augengneiss. The phengitic components produce significantly high activation energy estimates, in
the range 103–115 kcal/mol (431–481 kJ/mol) compared to estimates from the muscovite domain, in the range 54–61 kcal/mol
(226–255 kJ/mol). The estimated retentivity of the phengite implies that the ages measured are growth ages, since metamorphic
230 temperatures were less than the inferred closure temperatures. Therefore it appears that we have directly dated microstructures
produced during the Asteroussia event.

The garnet-mica schists that produced the Late Cretaceous Asteroussia ages were collected in the northern headland of the
Mylopotas Beach, Ios (Fig. 3). We have already noted that microstructural analysis of the garnet-mica schist IO17-03
demonstrated multiple episodes of white mica growth. The older grains in the deformation fabric 180 μm to 450 μm in
235 diameter, whereas the younger grains developed during or after later shear zone operation are elongate with dimensions range
50 μm to 90 μm , note that the older generation phengitic white micas were hand-picked for this sample.

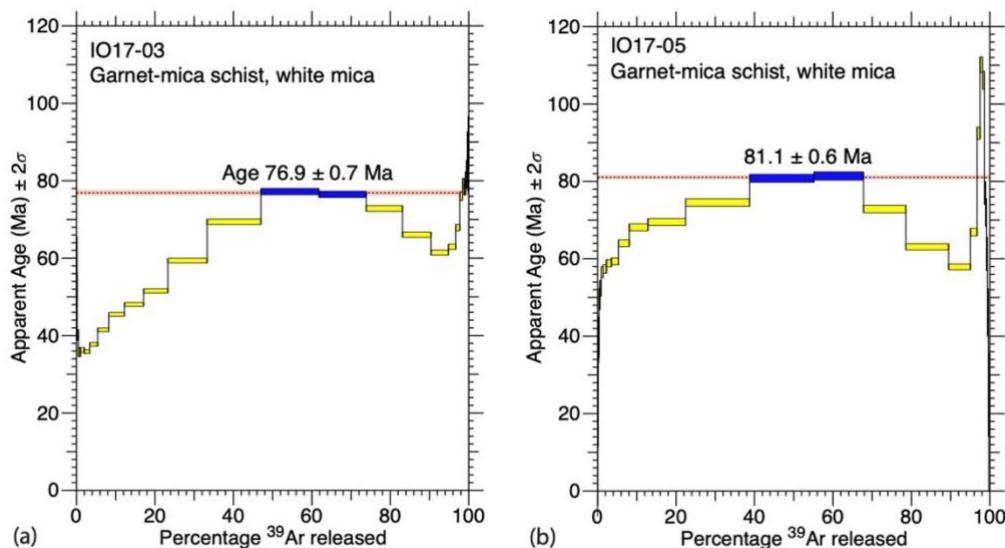
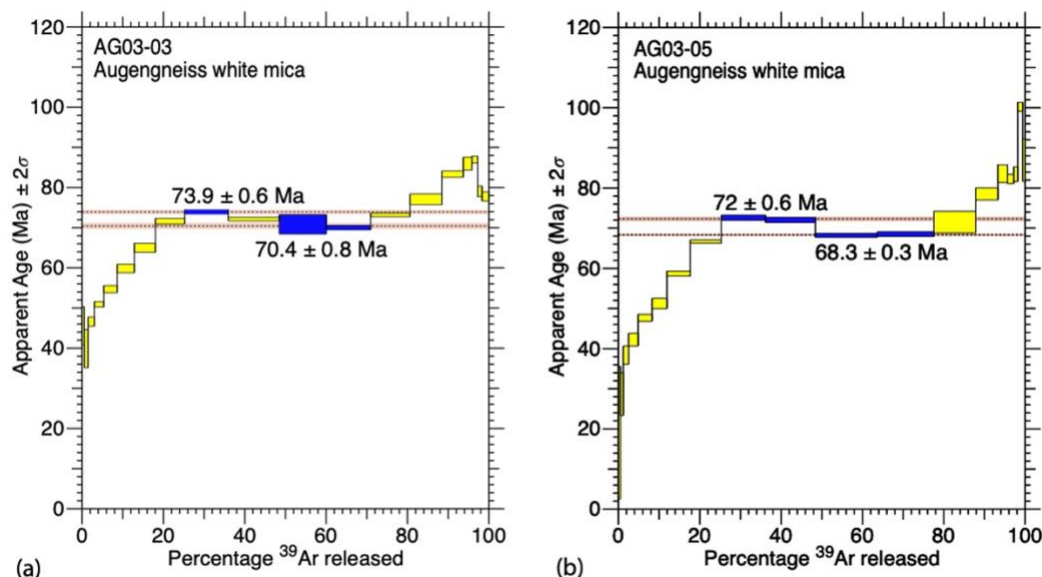


Figure 8: White mica age spectra from the structurally mid-level garnet-mica schist unit (IO17-03, IO17-05) produced Late Cretaceous age comparable to the Asteroussia event.

240

The $^{40}\text{Ar}/^{39}\text{Ar}$ results (Fig. 8a) suggest several different gas populations, comparable to microstructure observations, but the age spectrum is dominated by a phengitic partial plateau ('hump') with peak minimum age of 76.9 ± 0.7 Ma. Similarly, although the garnet-mica schist sample IO17-05 was collected near IO17-03, its pervasive deformation fabric comprised white micas recrystallised into narrow shear bands interlayered with dynamically recrystallised quartz. The phengitic partial plateau

245 of this sample produced a peak minimum age of 81.1 ± 0.6 Ma (Fig. 8b). The muscovite sub-spectrum records an event at 58.8 ± 1.5 Ma, a time comparable with estimates for the timing of the Δ_{1A} and Δ_{1B} Alpine events (Forster et al., 2015; Huet et al., 2009).



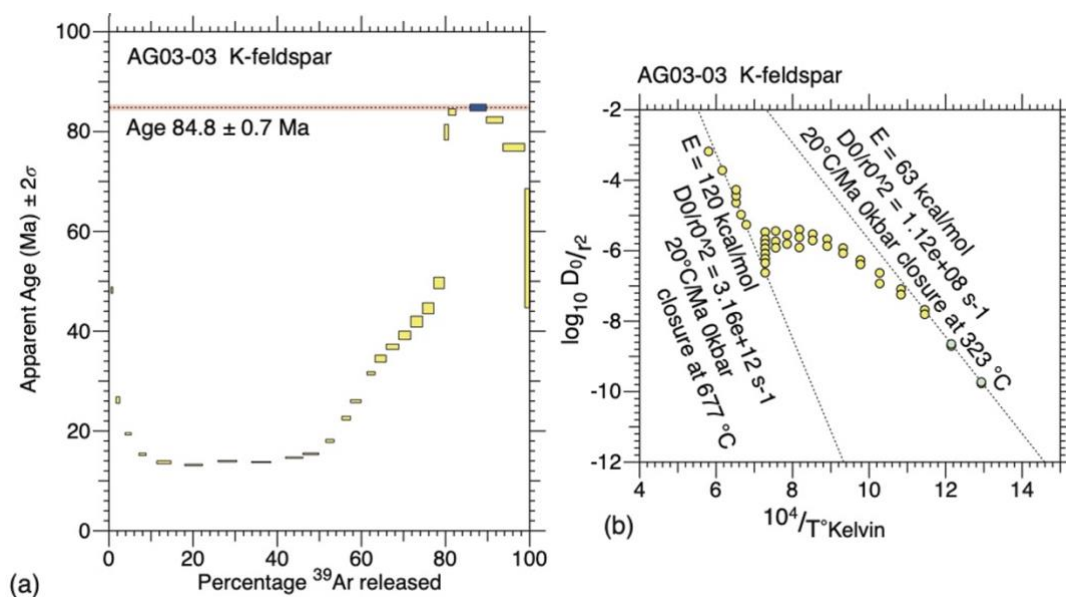
250 **Figure 9: White mica age spectra plot from the structurally lowest augengneiss core (AG03-03, AG03-05). The complex age spectra are a result of multiple argon populations degassing at different temperature during the step-heating experiment. The augengneiss basement was subjected to multiple deformation events, but a significant argon population of Late Cretaceous age is preserved.**

Augengneiss samples AG03-03 and AG03-05 were collected from structurally below the ductile shear zone that outcrops on the southern Mylopotas headland, and are microstructurally similar. They contain white mica deformation fabrics that
255 underwent minor recrystallisation during south-directed then north-directed shear zone operation. The method of asymptotes and limits in the AG03-03 white mica age spectrum yielded 74.0 Ma as the minimum oldest age, with an asymptote of 70.4 Ma as the maximum youngest age of the Late Cretaceous deformation fabric (Fig. 9a). White mica deformation fabrics in augengneiss AG03-05 reported a Late Cretaceous event with an upper limit at 72.3 ± 0.6 Ma and a lower limit at 68.3 ± 0.3 Ma representing the minimum and maximum ages respectively (Fig. 9b). From these data it is evident that the structurally
260 mid-level garnet-mica schist and the underlying augengneiss basement were subjected to complex deformation history with multiple events occurring from Early Cretaceous to Eocene (and potentially Miocene) time.

White mica and K-feldspar differ in their $^{40}\text{Ar}/^{39}\text{Ar}$ systematics and grow and respond differently to deformation. In AG03-03, Forster and Lister (2009) observe larger K-feldspars (porphyroclasts; 2000 – 6500 μm) and small K-feldspar grains (500-700



265 μm) interspersed between aligned white mica grains that recrystallised during later deformation. Forster et al. (2014) reported
that K-feldspars required analysis with isothermal steps so as to recognise contamination at each temperature increase in the
step heating procedure (i.e., isothermal steps being two or more heating steps at the same temperature). The first step is referred
to as a cleaning step and is not included in the interpretation of the spectrum. This same methodology is used on the K-feldspar
analysis in this study. Step-heating experiments on the K-feldspar samples produced saddle-shaped apparent age spectrum
270 with a lower limit at $\sim 13 \pm 0.1$ Ma (Fig. 10a). The last argon release steps produced a peak at 84.5 ± 0.8 Ma, comparable to
the date obtained from white mica from the same sample (Fig. 9a). The Arrhenius plot of this K-feldspar sample shows two
distinct argon diffusion domains (Fig. 10b). The K-feldspar porphyroclasts in the south Mylopotas augengneiss also preserved
complex deformation history, recording older Late Cretaceous events and younger middle Miocene events. The Arrhenius data
shows that these older domains were also highly retentive of argon, implying that potassium feldspar was replaced by
275 metamorphic and/or metasomatic events at those times.



280 **Figure 10:** a) K-feldspar age spectrum from the structurally lowest augengneiss core, this is an age spectrum with isothermal cleaning
steps removed. Note that there are younger ages identified from the age spectrum, the youngest deformation age observed is 13.2 ± 0.1 Ma from the lowest-part of the saddle-shaped spectrum. A minor asymptote dated 31.6 ± 0.3 Ma is also detected in the sample, but only prominent when isothermal cleaning steps are shown. These ages, however, are not Asteroussian and thus not shown in the figure. (b) Arrhenius plot of the same K-feldspar grain sample illustrating two argon diffusion domains with significantly different activation energy.



285 5 Discussion

5.1 Evidence of the Asteroussia event in the Ios lower plate

Microstructurally, our study conclusively identified the presence of more retentive phengite in a fabric that was later overprinted by dynamically recrystallized white mica and quartz. The earlier metamorphic fabrics formed under conditions that potentially reached eclogite facies. Our UHV ^{39}Ar diffusion experiments show that this phengite is highly retentive, thus
290 allowing preservation of the growth ages of white mica that formed during these earlier events. Thus, despite intense overprinting during Alpine deformation events, the Late Cretaceous argon populations were retained. This is consistent with the concept of an Argon Partial Retention Zone in which mineral grains undergo some partial resetting by diffusion, but where recrystallisation causes the most effects (Baldwin and Lister, 1998). Identification of the Late Cretaceous age in the Ios lower basement has been interpreted as a result of mixing (e.g., Andriessen et al., 1987). Instead of defining these dates as
295 “intermediate” ages due to excess radiogenic argon or simultaneous degas of the Alpine mica and the older Hercynian micas, here we have shown that these ages represent a period of Late Cretaceous deformation and metamorphism. Therefore the Ios basement may be part of the Asteroussia terrane. However, pressure-temperature estimates from phengites in the Ios lower plate record high pressure conditions, contrary to what has been observed in Asteroussia klippen across the Cyclades.

300 This suggests that more than one set of tectonic slices may have preserved Asteroussian ages. The Ios data is the first report of Asteroussia ages in a terrane of unmistakably Gondwanan affinity. The earliest reported argon age in Ios is a single K/Ar hornblende date reported to be Post-Hercynian (268 ± 27 Ma) by Andriessen et al. (1987) and Flansburg et al. (2019). It may be that the Asteroussian slices record a variety of metamorphic pressure conditions, with Tinos in the north recording peak metamorphic conditions at 650–750 MPa and 530–610 °C, Donoussa recording P-T conditions of 400–500 MPa and 600–650
305 °C (Kolodner et al., 1998), and slices in Crete recording 680–730 °C and 500–600 MPa (Be’eri-Shlevin et al., 2009; Kolodner et al., 1998; Langosch et al., 2000; Seidel et al., 1981). However, Be’eri-Shlevin et al. (2009) report that Anafi, in the central Cyclades reached P-T conditions at 200–600 MPa and >600 °C (Table 2).



TABLE 2 – PUBLISHED PEAK METAMORPHIC CONDITION ESTIMATES IN THE CYCLADES

Island	Published studies	Sample details/ methodology	Peak metamorphic condition
Tinos	Patzak et al., 1994 (as cited in Be'eri-Shlevin et al., 2009)	Interlayered amphibolite–paragneiss sequence in Akrotiri unit	650–750 MPa
			530–610 °C
Donoussa	Kolodner et al., 1998	N.A.	400–500 MPa 600–650 °C
Anafi	Be'eri-Shlevin 2009	EPMA analyses of garnet–biotite pairs from garnet-biotite paragneiss sample that occur as thin (1–2 m thick) layers within the structurally intermediate level of the Asteroussia Unit. Garnet–biotite temperatures were calculated using the equation of Ferry and Spear (1978). sample collected from a massive amphibolite exposure in the structurally intermediate level of the Asteroussia Unit edenite–tremolite (ed–tr) reactions edenite–richterite (ed–ri) reactions	Core of garnet & biotite ~720–740 °C* 200–600 MPa
			Rims of garnet & biotite 634–650 °C * 200–600 MPa
			*with error on temperatures in the range of ± 50 °C.
			677–726 °C 200–600 MPa
Crete	Seidel 1981	Peak metamorphism P-T conditions estimated from critical mineral assemblage of the outcrop of a variegated series consisting: tholeiitic ortho-amphibolites, para-amphibolites, andalusite and sillimanite-cordierite-garnet bearing mica schists, calcsilicate rocks, and marbles.	400–500 MPa maximum temperature ~ 700 °C



Crete (cont.)	Anderson and Smith, 1995 (as cited in Langosch et al., 2000)	Al-in- hornblende barometer Granodiorites of eastern Crete Granites and granodiorites of central Crete	100–200 MPa Maximum temperature = 700 °C 250–400 MPa Maximum temperature = 700 °C
	Koepke and Seidel, 1984 (as cited in Langosch et al., 2000)	Peak metamorphism P-T conditions estimated from metamorphic assemblages of quartz – plagioclase – K-feldspar – sillimanite – biotite – garnet – cordierite in pelitic paragneisses at central Crete	upper amphibolite facies: 400–600 MPa 650–700 °C
	Langosch, 1999 (as cited in Langosch et al., 2000)	Calculated by thermobarometric calibrations of Bhattacharya et al. (1988, 1992), Dwivedi et al. (1998), Koziol and Newton (1988) and Holland and Blundy (1994) Peak metamorphism P-T conditions estimated from metamorphic assemblages of (1) quartz – muscovite – chlorite – garnet – andalusite – plagioclase and (2) quartz – muscovite – biotite – staurolite – andalusite – plagioclase observed in metapelites of Asteroussian tectonic slices	680–730 °C 500–600 MPa lower amphibolite facies: ~ 550 °C 300 MPa

310 5.2 Tectonic implications

The nature of the tectonic processes that affected the evolution of the terranes accreted by the Hellenic subduction zone remains controversial (e.g., (Forster and Lister 2009; Forster et al., 2020) versus (Huet et al., 2009; Huet et al., 2011)). However, the current polemic seems misguided. The architecture of Tethyan orogenic belts, the Hellenides included, invariably involves a nappe- or a terrane-stack, and all terrane stacks are created by thrusting. However most if not all terrane stacks are also modified
 315 by later episodes of extension (e.g., Forster and Lister, 2009) leading to tectonic shuffling. It is no different in the Cyclades. The Cycladic archipelago preserves the results of the destruction of an extensive terrane-stack that extended from the Hellenides in Greece to the Taurus Mountains in Turkey (Gautier and Brun, 1994a, b; Kempler and Garfunkel, 1994;



McKenzie, 1977; Taymaz et al., 1991). The debate as to the nature of exhumation processes will not be resolved by a sole focus on the Cycladic eclogite-blueschist belt, as demonstrated in this paper.

320

The key questions surround the evolution of the terrane stack overall, rather than the details of the exhumation of an individual tectonic slice. The extrusion wedge (or forcible eduction) model suggests constant compression, resulting in the squeezing of softer material, so that it is extruded to the surface (Forster and Lister, 2008; Xypolias and Koukouvelas, 2001). The competing hypothesis, known as the tectonic mode switch or tectonic shuffle zone model, considers that thrust slices are exhumed by periods of crustal extension that take place in between episodes of crustal shortening caused by individual accretion events (Forster and Lister, 2009). Dispute arises because of the focus on the exhumation of the Cycladic eclogite-blueschist terranes, whereas the continuing nature of the orogenic process means that (without question) the subduction megathrust had to have episodically leapt southward every time a new terrane was accreted. As the African plate migrated northward, terranes were first subducted, then sliced from the subducting lithosphere by the advancing subduction megathrust, and thus accreted to the terrane stack (e.g., Lister et al., 2001; Lister and Forster, 2009).

330

For Ios, the question is how rollback of the subducting slab was able to throw the over-riding terrane-stack into horizontal extension immediately after the accretion of the Cycladic blueschist onto the Asteroussian terrane (Fig. 2), in particular given the requirement thereafter of a massive southwards leap of the outcrop of the active subduction megathrust. Previous work (e.g., Forster et al., 2020) has suggested that the Cycladic blueschist belt had already been largely exhumed before it was thrust over the Ios basement terrane in Late Eocene time (from ~38 Ma, Fig. 2a). A first period of extensional tectonism formed the Ios metamorphic core complex, and this had commenced by ~35 Ma, accelerating by the time of the Eocene–Oligocene transition. A second period of extensional tectonism then ensued, after the Oligocene–Miocene transition, with lithospheric extension triggering a major magmatic event, with intrusions in and through the core of younger metamorphic core complexes across the Cyclades (Kaey and Lister, 2002).

340



The Ios basement has been argued to be autochthonous, moving with Africa, and part of Gondwana (Flansburg et al., 2019; Keay et al., 2001; Kaey and Lister, 2002). Its accretion to the terrane stack is therefore likely to have been an event with considerable tectonic significance. The magnitude of the southward leap of the subduction megathrust is thus unlikely to have
345 been accomplished without the development of a new lithosphere-scale structure. There are two end-member options: one requiring that slab peels free from the subduction megathrust (Fig. 2c, after Brun and Faccenna, 2008) while the other requires a subduction jump and slab breakoff (Fig. 2d, cf. von Blanckenburg and Davies, 1995). Although the slab-peel model is consistent with enhanced heat flow during crustal stretching after the accretion event, Lister and Forster (2009) show that such a model requires the asthenosphere to be uplifted to sufficiently shallow levels that a period of major basaltic volcanism would
350 have taken place, with volumes comparable to those observed in some large igneous provinces. Sizova et al. (2019) also showed the “peel off” model (Brun and Faccenna, 2008) to be unlikely.

An alternative model must therefore be considered (e.g., Fig. 2d) involving slab boudinage and break off. This model also requires significant magmatism, since fluids rising from a devolatilising slab, leading to the appearance of arc volcanoes.
355 Necking and eventual break off of the subducting slab and formation of a new subduction zone (Fig. 2d) might be of sufficiently small scale to escape observation in models based on P-wave tomography.

5.3 Unresolved issues

We do not understand why the Asteroussia event is recorded in the top-most slices of the terrane stack outcropped in other
360 Cycladic islands, but is found only in the lower slice in Ios. Such architecture implies that the Cycladic eclogite-blueschist tectonics slices are ‘sandwiched’ between tectonic slices affected by the Asteroussia event, whereas on Crete the Asteroussia units are juxtaposed above the Vatos unit, the Arvi unit, the Pindos unit and the Tripoliz unit (e.g., Bonneau, 1984; Flansburg et al., 2019; Kneucker et al., 2015; Langosch et al., 2000; Martha et al., 2017; Martha et al., 2016, Palamakumbura et al., 2013; Seidel et al., 1976; Zulauf et al., 2002). This must have occurred sometime between Middle Oligocene–Lower Miocene time.
365 Laterally, the unit is connected to the eastern Alps in the west and the Lycian ophiolite nappes, the Menderes Massif and the Sakarya Zone in Turkey (Van Hinsbergen et al., 2020).



Some authors suggest that there are the tectonic slices outcropping on islands in the northwest (Andros, Tinos, Syros) are different to those on other islands such as Anafi, Nikoria, Donoussa, Ikaria and Crete (Altherr et al., 1994; Langosch et al., 2000; Martha et al., 2016). Arguments arise due to the difference in dates obtained (despite all being Late Cretaceous) and different results for geothermobarometry across islands with different lithologies and metamorphic facies (Kolodner et al., 1998; Langosch et al., 2000; Patzak et al., 1994; Seidel et al., 1976; Seidel et al., 1981; Yeung, 2019). Research in the upper and middle tectonic units in Tinos produced dates at 90-100 Ma and a peak metamorphic P-T estimate of 120 MPa at 450-500 °C (Avigad and Garfunkel, 1989; Avigad and Garfunkel, 1991; Bröcker and Franz, 1998; Patzak et al., 1994), whereas studies on Donoussa and Crete produced younger ages at 70-80 Ma and peak metamorphic P-T conditions at 300–600 MPa and 600-730 °C (Be'eri-Shlevin et al., 2009; Keay and Lister, 2002; Kolodner et al., 1998; Langosch et al., 2000; Seidel et al., 1976).

Our study reports metamorphic conditions with higher pressure, despite producing similar dates. Although the presence of phengite is wide-spread across the Ios lower plate, the highest pressures are inferred only in the garnet-mica schist unit and the Port Beach tectonic slice. With no evidence of higher pressures in the underlying augengneiss unit, it is possible that a more complex deformation and metamorphic history has been recorded in these intermediate slices in the Ios terrane stack.

These observations also reflect on a possible distinction between European and Gondwanan terranes, with evidence mostly preserved in the Alps and in the Pelagonian zone of Greece (Pourceau et al., 2013; Porkoláb et al., 2019; Regis et al., 2014; Thöni, 2006). Brown et al. (2014) reports evidence of Late Cretaceous intracontinental shear zone deformation across Africa, thus demonstrating that the ~70-80 Ma age is not limited to northern Tethys. Detrital zircon (DZ) analysis on preplutonic metasedimentary rocks in Ios lower plate by Flansburg et al. (2019) pushes tectono-magmatic histories of the southern Cyclades further in time to early Cenozoic. They noted a striking resemblance between their DZ age spectra from Ios lower plate to exposures on Crete, northern and central Peloponnese, the northern Hellenides and the siliciclastic cover sequence of the Menderes massif in western Turkey (Flansburg et al., 2019). Comparing these Ios DZ age spectra to those from northeast Africa and Arabia, they confirmed that the Cycladic basement terrane (outcropped in Ios lower plate) have a distinct peri-



Gondwanan affinity (Flansburg et al., 2019). This led them to propose a tectonic model where the terrane was located along the northern margin of Gondwana in early Paleozoic and experienced pluton emplacement between ~335 and ~305 Ma in an arc setting (Flansburg et al., 2019).

395

Tectonic reconstructions by Van Hinsbergen et al. (2020) demonstrated that major continental-scale events occurred across Eurasia and Gondwana from Late Jurassic–Late Cretaceous time. These global tectonic events involve continental-scale deformation such as the formation of the Alpine Tethys with microcontinents tearing from the south coast of Europe. In their reconstruction model, the Ios basement, along with other tectonic units in the Cycladic islands and Crete, are all part of a subducted Greater Adria continental ribbon. While our island-scale study cannot contribute to the discussion on whether Greater Adria was a single continental landmass or made up of several large islands, it is evident that Late Cretaceous deformation is wide-spread in both the European and Gondwana terranes.

400

Distinguishing European versus Gondwanan terranes in the Central Aegean and greater Mediterranean area will remain difficult. One central argument is the number of oceans present in the ‘greater Tethys seaway’ between Europe, Africa and potentially Adria at Mesozoic and associated tectonic evolution (e.g., Channell and Kozur, 1997; Kiliyas et al., 2010; Robertson et al., 2013). This argument mainly concerns the paleogeography of the Pelagonian unit outcropped in mainland Greece. It is thus of interest that evidence for Late Cretaceous ages is reported from white mica deformation fabrics isolated from the northern end of the upper Pelagonian unit (e.g., Kiliyas et al., 2010; Robertson et al., 2013). The Pelagonian unit may have been a continental ribbon (or micro-continent) separating two Tethyan realms: the Vardar Ocean in the northeast and the Pindos (or even Cyclades) Ocean in the southwest (e.g., Channell and Kozur, 1997; Robertson et al., 2013). Such models imply high pressure metamorphism in the Pelagonian unit as the result of the attempted subduction of the continental ribbon (Robertson et al., 2013). Other reconstructions consider the Pelagonian unit as the eastern-most unit of a continental Adria terrane, adjacent to a single north-eastern oceanic basin (the Vardar Ocean) e.g., (Bortolotti et al., 2013; Ferriere et al., 2012; Kiliyas et al., 2010; Palamakumbura et al., 2013). These researchers disagree with the concept of an distinct Pindos Ocean both in Triassic and in Jurassic time (Kiliyas et al., 2010).

410

415



6 Conclusion

Our study reports evidence of a Late Cretaceous Asteroussia event (70–80 Ma) in the Gondwana originated lower plate of Ios. Accretion of the Asteroussia terrane is a major event in the Aegean tectonic history. This required a (250–300 km) southward jump of the subduction megathrust. Renewed rollback after the accretion event triggered Oligocene extension and facilitated
420 the exhumation of the Asteroussia terrane as the Ios metamorphic core complex.

Data availability

$^{40}\text{Ar}/^{39}\text{Ar}$ geochronology results of two augengneiss samples (AG03-03, AG03-05) were published in Forster and Lister (2009) and re-examined in this study. All new data collected in this study and presented in this article are provided in text and in the
425 Masters' thesis of Sonia Yeung submitted for her Masters' programme to the Research School of Earth Sciences, Australian National University.

Team list

Sonia Yeung¹, Marnie Forster¹, Emmanuel Skourtsos², Gordon Lister¹

¹Structure Tectonics Team, Research School of Earth Sciences, Australian National University, Canberra, 2601 Australia

430 ²Section of Dynamic, Tectonic and Applied Geology, Department of Geology and Geoenvironment, National and Kapodistrian University of Athens, Athens 157 72, Greece

Author contribution

All authors contributed to the writing of the manuscript and its conceptualisation. The paper extends part of a Master's thesis
435 by Sonia Yeung, supervised by Marnie Forster and Gordon Lister.



Disclaimer

The article includes a minor part of the Masters' Thesis of Sonia Yeung submitted for her Masters' programme to the Research School of Earth Sciences, Australian National University.

440 Conflicts of Interest

The authors declare that they have no conflicts of interest.

Funding Statement

Research support were provided by the Australian Research Council Discovery Project [grants numbers: DP120103554 “A unified model for the closure dynamics of ancient Tethys constrained by Geodesy, Structural Geology, Argon Geochronology and Tectonic Reconstruction” and LP130100134 “Where to find giant porphyry and epithermal gold and copper deposits”].
445 Sample Irradiations were paid by the Research School of Earth Science argon facility, Australian National University and facilitated by the University of California Davis McClellan Nuclear Research Centre, CA, US.

Acknowledgments

450 The authors acknowledge the microprobe mineral chemistry analysis was performed in the facilities, with the scientific and technical assistance in Microscopy Australia at the Centre of Advanced Microscopy, The Australian National University. Sample Irradiations for $^{40}\text{Ar}/^{39}\text{Ar}$ geochronology were facilitated by the University of California Davis McClellan Nuclear Research Centre, CA, US. Argon analyses and microstructure analyses were performed at the Research School of Earth Sciences Laboratories at the Australian National University. Davood Vasegh in the Argon Lab provided technical assistance
455 for the step heating experiments, Shane Paxton in the mineral separation facility provided technical assistance for sample preparation. Step-heating experimental results for $^{40}\text{Ar}/^{39}\text{Ar}$ geochronology were analysed using programmes *eArgon* and *MacArgon* developed by G.S. Lister (<http://rses.anu.edu.au/tectonics/programs/>).



References

- Altherr, R., Kreuzer, H., and Lenz, H.: Further Evidence for a Late Cretaceous Low-pressure, *Chem. Erde*, 54, 319-328, 1994.
- 460 Andriessen, P., Banga, G., and Hebeda, E.: Isotopic age study of pre-Alpine rocks in the basal units on Naxos, Sikinos and Ios, Greek Cyclades, *Geologie en Mijnbouw*, 66, 3-14, 1987.
- Avigad, D. and Garfunkel, Z.: Low-angle faults above and below a blueschist belt—Tinos Island, Cyclades, Greece, *Terra Nova*, 1, 182-187, 1989.
- Avigad, D. and Garfunkel, Z.: Uplift and exhumation of high-pressure metamorphic terrains: the example of the Cycladic
- 465 blueschist belt (Aegean Sea), *Tectonophysics*, 188, 357-372, 1991.
- Baldwin, S. L. and Lister, G. S.: Thermochronology of the South Cyclades Shear Zone, Ios, Greece: Effects of ductile shear in the argon partial retention zone, *Journal of Geophysical Research: Solid Earth*, 103, 7315-7336, 1998.
- Be'eri-Shlevin, Y., Avigad, D., and Matthews, A.: Granitoid intrusion and high temperature metamorphism in the Asteroussia Unit, Anafi Island (Greece): Petrology and geochronology, *Israel Journal of Earth Sciences*, 58, 2009.
- 470 Bonneau, M.: LA NAPPE METAMORPHIQUE DE L'ASTEROUSSIA, LAMBEAU D'AFFINITES PELAGONIENNES CHARRIE JUSQUE SUR LA ZONE DE TRIPOLITZA DE LA CRETE MOYENNE (GRECE, 1972. 1972.
- Bonneau, M.: Correlation of the Hellenide nappes in the south-east Aegean and their tectonic reconstruction, *Geological Society, London, Special Publications*, 17, 517-527, 1984.
- Bortolotti, V., Chiari, M., Marroni, M., Pandolfi, L., Principi, G., and Saccani, E.: Geodynamic evolution of ophiolites from
- 475 Albania and Greece (Dinaric-Hellenic belt): one, two, or more oceanic basins?, *International Journal of Earth Sciences*, 102, 783-811, 2013.
- Bröcker, M. and Franz, L.: Rb–Sr isotope studies on Tinos Island (Cyclades, Greece): additional time constraints for metamorphism, extent of infiltration-controlled overprinting and deformational activity, *Geological Magazine*, 135, 369-382, 1998.
- 480 Brocker, M. and Franz, L.: Dating metamorphism and tectonic juxtaposition on Andros Island (Cyclades, Greece): results of a Rb–Sr study, *Geological Magazine*, 143, 609-620, 2006.



- Brown, R., Summerfield, M., Gleadow, A., Gallagher, K., Carter, A., Beucher, R., and Wildman, M.: Intracontinental deformation in southern Africa during the Late Cretaceous, *Journal of African Earth Sciences*, 100, 20-41, 2014.
- Brun, J.-P. and Faccenna, C.: Exhumation of high-pressure rocks driven by slab rollback, *Earth and Planetary Science Letters*, 485 272, 1-7, 2008.
- Channell, J. and Kozur, H.: How many oceans? Meliata, Vardar and Pindos oceans in Mesozoic Alpine paleogeography, *Geology*, 25, 183-186, 1997.
- Dürr, S.: THE MEDIAN AEGEAN CRYSTALLINE BELT: STRALIGRAPHY STRUCTURE, METAMORPHISM, MAGMATISM, 1978. 1978.
- 490 Ferriere, J., Chanier, F., and Ditbanjong, P.: The Hellenic ophiolites: eastward or westward obduction of the Maliac Ocean, a discussion, *International Journal of Earth Sciences*, 101, 1559-1580, 2012.
- Flansburg, M. E., Stockli, D. F., Poulaki, E. M., and Soukis, K.: Tectono-magmatic and stratigraphic evolution of the Cycladic basement, Ios Island, Greece, *Tectonics*, 38, 2291-2316, 2019.
- Forster, M., Armstrong, R., Kohn, B., Lister, G., Cottam, M., and Suggate, S.: Highly retentive core domains in K-feldspar 495 and their implications for $^{40}\text{Ar}/^{39}\text{Ar}$ thermochronology illustrated by determining the cooling curve for the Capoas Granite, Palawan, The Philippines, *Australian Journal of Earth Sciences*, 62, 883-902, 2015.
- Forster, M., Koudashev, O., Nie, R., Yeung, S., and Lister, G.: $^{40}\text{Ar}/^{39}\text{Ar}$ thermochronology in the Ios basement terrane resolves the tectonic significance of the South Cyclades Shear Zone, *Geological Society, London, Special Publications*, 487, 291-313, 2020.
- 500 Forster, M. and Lister, G.: Detachment faults in the Aegean core complex of Ios, Cyclades, Greece, *Geological Society, London, Special Publications*, 154, 305-323, 1999a.
- Forster, M. and Lister, G.: The interpretation of $^{40}\text{Ar}/^{39}\text{Ar}$ apparent age spectra produced by mixing: application of the method of asymptotes and limits, *Journal of Structural Geology*, 26, 287-305, 2004.
- Forster, M. and Lister, G.: Tectonic sequence diagrams and the structural evolution of schists and gneisses in multiply 505 deformed terranes, *Journal of the Geological Society*, 165, 923-939, 2008.



- Forster, M. and Lister, G.: Core-complex-related extension of the Aegean lithosphere initiated at the Eocene-Oligocene transition, *Journal of Geophysical Research: Solid Earth*, 114, 2009.
- Forster, M. and Lister, G.: Argon enters the retentive zone: reassessment of diffusion parameters for K-feldspar in the South Cyclades Shear Zone, Ios, Greece, Geological Society, London, Special Publications, 332, 17-34, 2010.
- 510 Forster, M., Lister, G., and Lennox, P.: Dating deformation using crushed alkali feldspar: $^{40}\text{Ar}/^{39}\text{Ar}$ geochronology of shear zones in the Wyangala Batholith, NSW, Australia, *Australian Journal of Earth Sciences*, 61, 619-629, 2014.
- Forster, M. A. and Lister, G. S.: Separate episodes of eclogite and blueschist facies metamorphism in the Aegean metamorphic core complex of Ios, Cyclades, Greece, Geological Society, London, Special Publications, 164, 157-177, 1999b.
- Gautier, P. and Brun, J.-P.: Ductile crust exhumation and extensional detachments in the central Aegean (Cyclades and Evvia
515 Islands), *Geodinamica Acta*, 7, 57-85, 1994.
- Gautier, P. and Brun, J.-P.: Crustal-scale geometry and kinematics of late-orogenic extension in the central Aegean (Cyclades and Ewia Island), *Tectonophysics*, 238, 399-424, 1994.
- Huet, B., Labrousse, L., and Jolivet, L.: Thrust or detachment? Exhumation processes in the Aegean: Insight from a field study on Ios (Cyclades, Greece), *Tectonics*, 28, 2009.
- 520 Huet, B., Le Pourhiet, L., Labrousse, L., Burov, E., and Jolivet, L.: Post-orogenic extension and metamorphic core complexes in a heterogeneous crust: the role of crustal layering inherited from collision. Application to the Cyclades (Aegean domain), *Geophysical Journal International*, 184, 611-625, 2011.
- Keay, S. and Lister, G.: African provenance for the metasediments and metaigneous rocks of the Cyclades, Aegean Sea, Greece, *Geology*, 30, 235-238, 2002.
- 525 Keay, S., Lister, G., and Buick, I.: The timing of partial melting, Barrovian metamorphism and granite intrusion in the Naxos metamorphic core complex, Cyclades, Aegean Sea, Greece, *Tectonophysics*, 342, 275-312, 2001.
- Kempler, D. and Garfunkel, Z.: Structures and kinematics in the northeastern Mediterranean: a study of an irregular plate boundary, *Tectonophysics*, 234, 19-32, 1994.
- Kilias, A., Frisch, W., Avgerinas, A., Dunkl, I., Falalakis, G., and Gawlick, H.-J.: Alpine architecture and kinematics of
530 deformation of the northern Pelagonian nappe pile in the Hellenides, *Austrian Journal of Earth Sciences*, 103, 4-28, 2010.



- Kneucker, T., Dörr, W., Petschick, R., and Zulauf, G.: Upper crustal emplacement and deformation of granitoids inside the Uppermost Unit of the Cretan nappe stack: constraints from U–Pb zircon dating, microfabrics and paleostress analyses, *International Journal of Earth Sciences*, 104, 351-367, 2015.
- Kolodner, K., Matthews, A., Avigad, D., and Garfunkel, Z.: High temperature Alpine metamorphism in the eastern part of the Attic-Cycladic Massive (Greece) and its implications for early orogenesis, 1998, 55-55.
- Langosch, A., Seidel, E., Stosch, H.-G., and Okrusch, M.: Intrusive rocks in the ophiolitic mélangé of Crete—Witnesses to a Late Cretaceous thermal event of enigmatic geological position, *Contributions to Mineralogy and Petrology*, 139, 339-355, 2000.
- Lister, G. and Forster, M.: Tectonic mode switches and the nature of orogenesis, *Lithos*, 113, 274-291, 2009.
- Lister, G., Forster, M. A., and Rawling, T. J.: Episodicity during orogenesis, Geological Society, London, Special Publications, 184, 89-113, 2001.
- Lister, G. S. and Baldwin, S. L.: Modelling the effect of arbitrary PTt histories on argon diffusion in minerals using the MacArgon program for the Apple Macintosh, *Tectonophysics*, 253, 83-109, 1996.
- Makris, J., Papoulia, J., Papanikolaou, D., and Stavrakakis, G.: Thinned continental crust below northern Evoikos Gulf, central Greece, detected from deep seismic soundings, *Tectonophysics*, 341, 225-236, 2001.
- Makris, J. and Veis, R.: Crustal structure of the central Aegean Sea and the islands of Evia and Crete, Greece, obtained by refractive seismic experiments, *Journal of Geophysics* | IF 32.18, 42, 329-341, 1976.
- Martha, S. O., Dörr, W., Gerdes, A., Krahl, J., Linckens, J., and Zulauf, G.: The tectonometamorphic and magmatic evolution of the Uppermost Unit in central Crete (Melambes area): constraints on a Late Cretaceous magmatic arc in the Internal Hellenides (Greece), *Gondwana Research*, 48, 50-71, 2017.
- Martha, S. O., Dörr, W., Gerdes, A., Petschick, R., Schastok, J., Xypolias, P., and Zulauf, G.: New structural and U–Pb zircon data from Anafi crystalline basement (Cyclades, Greece): constraints on the evolution of a Late Cretaceous magmatic arc in the Internal Hellenides, *International Journal of Earth Sciences*, 105, 2031-2060, 2016.
- Massonne, H.-J. and Schreyer, W.: Phengite geobarometry based on the limiting assemblage with K-feldspar, phlogopite, and quartz, *Contributions to Mineralogy and Petrology*, 96, 212-224, 1987.



- McKenzie, D.: Surface deformation, gravity anomalies and convection, *Geophysical Journal International*, 48, 211-238, 1977.
- Palamakumbura, R. N., Robertson, A. H., and Dixon, J. E.: Geochemical, sedimentary and micropaleontological evidence for a Late Maastrichtian oceanic seamount within the Pindos ocean (Arvi Unit, S Crete, Greece), *Tectonophysics*, 595, 250-262, 2013.
- 560 Passchier, C. W. and Simpson, C.: Porphyroclast systems as kinematic indicators, *Journal of Structural Geology*, 8, 831-843, 1986.
- Patrick, B.: High-pressure-low-temperature metamorphism of granitic orthogneiss in the Brooks Range, northern Alaska, *Journal of Metamorphic Geology*, 13, 111-124, 1995.
- Patzak, M., Okrusch, M., and Kreuzer, H.: The Akrotiri Unit on the island of Tinos, Cyclades, Greece: Witness to a lost terrane
565 of Late Cretaceous age.(with 18 figures and 8 tables in the text), *Neues Jahrbuch für Geologie und Paläontologie-Abhandlungen*, 194, 211-252, 1994.
- Pe-Piper, G. and Photiades, A.: Geochemical characteristics of the Cretaceous ophiolitic rocks of Ikaria island, Greece, *Geological Magazine*, 143, 417-429, 2006.
- Porkoláb, K., Willingshofer, E., Sokoutis, D., Creton, I., Kostopoulos, D., and Wijbrans, J.: Cretaceous-Paleogene tectonics
570 of the Pelagonian zone: Inferences from Skopelos island (Greece), *Tectonics*, 38, 1946-1973, 2019.
- Pourteau, A., Sudo, M., Candan, O., Lanari, P., Vidal, O., and Oberhänsli, R.: Neotethys closure history of Anatolia: insights from 40Ar - 39Ar geochronology and P-T estimation in high-pressure metasedimentary rocks, *Journal of Metamorphic Geology*, 31, 585-606, 2013.
- Regis, D., Rubatto, D., Darling, J., Cenko-Tok, B., Zucali, M., and Engi, M.: Multiple metamorphic stages within an eclogite-
575 facies terrane (Sesia Zone, Western Alps) revealed by Th-U-Pb petrochronology, *Journal of Petrology*, 55, 1429-1456, 2014.
- Ring, U., Thomson, S. N., and BRÖCKER, M.: Fast extension but little exhumation: the Vari detachment in the Cyclades, Greece, *Geological Magazine*, 140, 245-252, 2003.
- Ring, U., Will, T., Glodny, J., Kumerics, C., Gessner, K., Thomson, S., Güngör, T., Monié, P., Okrusch, M., and Drüppel, K.:
580 Early exhumation of high-pressure rocks in extrusion wedges: Cycladic blueschist unit in the eastern Aegean, Greece, and Turkey, *Tectonics*, 26, 2007.



- Robertson, A. H., Trivić, B., Đerić, N., and Bucur, I. I.: Tectonic development of the Vardar ocean and its margins: Evidence from the Republic of Macedonia and Greek Macedonia, *Tectonophysics*, 595, 25-54, 2013.
- Seidel, E., Okrusch, M., Kreuzer, H., Raschka, H., and Harre, W.: Eo-alpine metamorphism in the uppermost unit of the Cretan nappe system—Petrology and geochronology, *Contributions to Mineralogy and Petrology*, 76, 351-361, 1981.
- 585 Seidel, E., Okrusch, M., Kreuzer, H., Raschka, H., and Harre, W.: Eo-alpine metamorphism in the uppermost unit of the Cretan nappe system—Petrology and geochronology, *Contributions to Mineralogy and Petrology*, 76, 351-361, 1981.
- Sizova, E., Hauzenberger, C., Fritz, H., Faryad, S. W., and Gerya, T.: Late orogenic heating of (ultra) high pressure rocks: slab rollback vs. slab breakoff, *Geosciences*, 9, 499, 2019.
- Taymaz, T., Jackson, J., and McKenzie, D.: Active tectonics of the north and central Aegean Sea, *Geophysical Journal International*, 106, 433-490, 1991.
- 590 Thöni, M.: Dating eclogite-facies metamorphism in the Eastern Alps—approaches, results, interpretations: a review, *Mineralogy and Petrology*, 88, 123-148, 2006.
- Van Hinsbergen, D. J., Torsvik, T. H., Schmid, S. M., Mañenco, L. C., Maffione, M., Vissers, R. L., Gürer, D., and Spakman, W.: Orogenic architecture of the Mediterranean region and kinematic reconstruction of its tectonic evolution since the Triassic, *Gondwana Research*, 81, 79-229, 2020.
- 595 Vandenberg, L. C. and Lister, G. S.: Structural analysis of basement tectonites from the Aegean metamorphic core complex of Ios, Cyclades, Greece, *Journal of Structural Geology*, 18, 1437-1454, 1996.
- Velde, B.: Si⁴⁺ content of natural phengites, *Contributions to Mineralogy and Petrology*, 14, 250-258, 1967.
- von Blanckenburg, F. and Davies, J. H.: Slab breakoff: a model for syncollisional magmatism and tectonics in the Alps, *Tectonics*, 14, 120-131, 1995.
- 600 Xypolias, P. and Koukouvelas, I.: Kinematic vorticity and strain rate patterns associated with ductile extrusion in the Chelmos Shear Zone (External Hellenides, Greece), *Tectonophysics*, 338, 59-77, 2001.
- YEUNG, H.S.: Timing of Central Aegean tectonic events during Tethys Ocean Closure. [MSc (adv.) thesis]: Australian National University, Australia, 2019



- 605 Zulauf, G., Kowalczyk, G., Krahl, J., Petschick, R., and Schwanz, S.: The tectonometamorphic evolution of high-pressure low-temperature metamorphic rocks of eastern Crete, Greece: constraints from microfabrics, strain, illite crystallinity and paleodifferential stress, *Journal of Structural Geology*, 24, 1805-1828, 2002.